Studies on Fracture Behavior of Tough PA6/PP Blends

M. HEINO,[1] P. HIETAOJA,[1] J. SEPPÄLÄ,[1] T. HARMIA,[2] K. FRIEDRICH[2]

[1] Helsinki University of Technology, Department of Chemical Engineering, Kemistintie 1, FIN-02150 Espoo, Finland

[2] Institut für Verbundwerkstoffe GmbH, Erwin-Schrödinger-Strasse Geb. 58, D-67663 Kaiserslautern, Germany

Received 4 September 1996; accepted 3 May 1997

ABSTRACT: Fracture toughness of injection-molded PA6/PP blends compatibilized with SEBS-*g*-MA was studied using deeply double-edge notched tension (DDENT) specimens according to the essential work of fracture procedure. The fracture mechanical studies also included tensile impact tests on the DDENT specimens and characterization of the fracture surfaces by electron microscopy. The results were compared with those of traditional tensile tests and Izod impact tests on single-edge notched samples, and the sensibility of the methods was evaluated. Effects of sample position, ligament length, testing direction, and test speed were studied as well. It was found that the essential work of fracture concept, earlier applied to thin sheets, can also be applied to injection-molded tough blends. High deformation of the skin may, however, interfere with the measurements and cause a "tail" in the load-deformation curves. The plastic work of fracture (w_p) was found to correlate with the impact strength, and thus, it described the toughness. The highest values for work of fracture were recorded for the compatibilized blend with a PA6/PP ratio of 80/20. The essential work of fracture (w_e) in turn increased with increasing PA6 content and behaved like tensile strength. The test speed was found to affect the fracture behavior substantially: differences between the materials were more pronounced in high-speed tensile impact tests, which revealed signs of cavitation in addition to large-scale plastic deformation for the tough PA6-rich blend compositions. J Appl Polym Sci **66:** 2209–2220, 1997

Key words: fracture toughness; essential work of fracture; plastic work of fracture; PA6/PP blend; compatibilization; morphology

INTRODUCTION

Blending two or more thermoplastic polymers is a feasible way to upgrade the properties of a certain polymer or to achieve totally new and unique property combinations. Blending of different polymers, which often are immiscible in each other, results in a two-phase morphology with the minor phase in the form of spherical droplets, platelets, or fibers. In some cases, cocontinuous network-like structures are formed as well. As demonstrated with many blends, the morphology (that is, the size and shape) of the minor phase and the interfacial adhesion between the polymers play a crucial role in determining the properties of the blend. The basic material parameters affecting the flow-induced morphology are blend composition, ratio of the viscosities, and melt elasticities of the blended polymers, as well as the interfacial tension. The processing conditions, including melt temperature, residence time, shear rate, and elongational drawing, have a significant effect as well. Morphology control is thus of great importance for all blend

Correspondence to: M. Heino.

Contract grant sponsor: Finnish Academy, Technology Development Center of Finland (TEKES).

Contract grant sponsor: Deutscher Akademischer Austausch Dienst; contract grant number: 313/SF-PPP.

Journal of Applied Polymer Science, Vol. 66, 2209–2220 (1997)
 CCC 0021-8995/97/122209-12

properties, and unusual synergistic properties may be achieved through the formation of specific morphologies and effective compatibilization.[1–5]

Blends of polypropylene (PP) and polyamides (PA) have been of considerable interest to researchers in recent years. With the aim of combining the good mechanical and thermal properties of PAs with the moisture insensitivity of PP, studies have been focused, among other things, on the structure–property relationships, morphology evolution, and compatibilization of the blends. Because the blends of standard PA and PP are brittle, compatibilization is necessary to achieve tough blend compositions.[2,6–17]

Particularly tough PA/PP blends have been achieved by adding maleated poly(styrene-*block*-(ethylene-butylene)-*block*-styrene), that is, SEBS-*g*-MA, as a compatibilizer. Holsti-Miettinen et al.[6,7] found that at a specific composition of PA6/PP at a weight ratio of 80/20, the addition of 10 wt % of SEBS-*g*-MA led to unexpected, dramatically improved toughness. The origin of this super toughness was elucidated by morphology analysis with transmission electron microscopy (TEM), which showed a unique morphology consisting of a continuous elastomer phase with finely dispersed PA6 inclusions. Actually, PA6 and SEBS-*g*-MA appeared to form a kind of cocontinuous network and PP formed an additional dispersed phase. Recently, Ikkala et al.[8] clarified the morphological origin of the supertoughness of this particular blend composition and found similar behavior in corresponding PA6/HDPE/SEBS-*g*-MA blends. In contrast to rubber-toughened thermoplastics, where the basic criteria of toughening such as size and distance of the rubber particles and their adhesion to the matrix are well known,[18–21] the factors determining toughness in multiphase polymer blends exhibiting complex morphologies are not well understood. To understand these interactions more profoundly requires fracture mechanical studies.

In general, the characterization of toughness of highly ductile polymers and polymer blends is a difficult task, which has, however, been successfully handled by applying both linear elastic fracture mechanics and plastic or postyield fracture mechanics.[22,23] One approach to determining the material toughness, so far applied mainly to thin sheets,[24,25] is the essential work of fracture procedure, which divides the total work of fracture per unit area (w_f) into two parts: the essential work (w_e) which is needed to fracture the polymer in its process zone and the plastic work dissipation per unit volume (w_p), which is the work related to other plastic deformations.[26] In view of the straightforward way of determining the w_e as well as the w_p, by plotting the work of fracture as a function of the ligament length, it seemed to us that this method might offer an accurate and efficient way of determining the "toughness" of ductile injection-molded blends.

Accordingly, the aim of our study was to characterize the toughness of four different PA6/PP blend compositions by applying the essential work of fracture procedure[26] on deeply double-edge notched (DDENT) specimens and then to compare the results with those of traditional tensile tests and Charpy or Izod impact tests on single-edge notched samples. The idea was thus to study the applicability of the methods to describe differences in fracture toughness between the selected blends. The fracture mechanical studies involved both tensile and tensile impact tests on samples taken from different parts of the injection-molded plates. Effects of sample position, ligament length, testing direction, and test speed were studied as well. In addition, the fracture surfaces generated in the tests were characterized by scanning electron microscopy (SEM).

EXPERIMENTAL

Materials

The PP grade was VC12 33B (Melt Flow Index [MFI]: 12 g/10 min at 230°C and 2.16 kg), supplied by Borealis Polymers, and the polyamide (PA6) was Ultramid B3S (MFI: 150 g/10 min at 275°C and 5 kg), produced by BASF. Poly(styrene-*block*-(ethylene–butylene)-*block*-styrene) elastomer functionalized with maleic anhydride (SEBS-*g*-MA; Kraton FG1901X from Shell; MFI: 18 g/10 min at 200°C and 5 kg) served as the compatibilizer. The content of styrene was 28 wt % and that of the grafted MA about 2 wt %, according to the manufacturer. The blend compositions studied are presented in Table I, which also shows the fracture mechanical results.

Blending and Injection Molding

PA6 was dried at 85°C overnight in a dehumidifying dryer before blending. The blends were prepared with a Werner & Pfleiderer ZSK 25 M9 corotating twin-screw extruder at 245°C with a screw speed of 200 rpm and a throughput of 6 kg/h. The

Table I Essential (w_e) and Plastic Work of Fracture (w_p) of Different Blend Compositions and Sample Positions Determined by Low-Speed Tensile Test (2 mm/min)

Blend Code	Composition PA6/PP/Comp.	Position	w_e (kJ/m^2)	w_p (MJ/m^3)
1	54/36/10	1	17.3	105.0
		2	5.1	152.0
2	72/18/10	1	22.0	160.0
		2	20.8	124.0
		3	17.6	184.0
2A	80/20/0	1	20.5	4.0
		2	22.0	4.6
		3	21.9	5.8
3	90/0/10	1	31.1	137.0
		2	32.9	177.0
		3	35.3	183.0

extrudate was immediately quenched in a water bath and pelletized. After drying, the blends were injection molded with an Engel ES 200/40 to standard tensile and impact test specimens and 2-mm thin plates (80 × 80 mm). The temperature of the barrel was about 245°C and that of the mold was 50°C.

Characterization

Because PA is highly sensitive to moisture, the samples were dried for 16 h at 80°C in a dehumidifying dryer before testing. Tensile properties were characterized with an Instron 4204 with a test speed of 50 mm/min (1 mm/min for modulus), according to standard ISO 527. Notched Izod impact tests were made on standard single-edge notched specimens (dimensions: 4 × 10 × 80 mm) with a Zwick 5102, according to ISO 179-1982.[6]

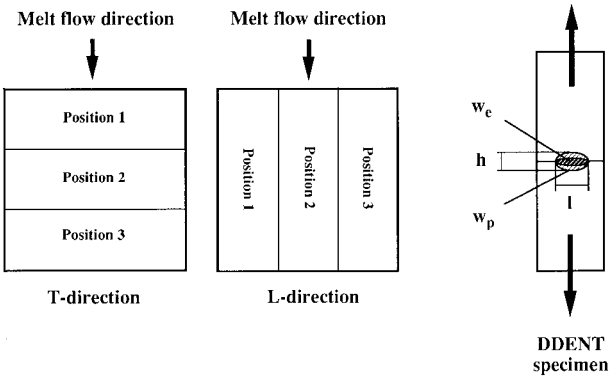

Figure 1 Description of (a) sample positions and (b) the DDENT test specimen.

The fracture mechanical characterization consisted of tensile and tensile impact tests on the DDENT specimens (Fig. 1) and microscopic analysis of the fracture surfaces generated in these tests. Three rectangular specimens (26 × 80 mm of 2-mm thickness) were cut from each injection-molded plate, and V notches were made on both sides of each specimen. The V notches were subsequently extended by a minimum of 1 mm by pressing the base of the notch with a sharp blade. It is important that the two notches are directly opposite each other and that they are equal in length.

Tensile properties of the DDENT specimens were characterized with a Zwick 1485 with a test speed of 2 mm/min (slow), according to the procedure described previously.[24] The load-deformation traces were recorded, and the total work of fracture (W_f) was calculated. Samples representing three different positions in both flow (L) and transversal (T) directions of the injection-molded plates were characterized. Studies were made with four different ligament lengths (l), and three parallel specimens were tested in each case.

Tensile impact tests were made on DDENT specimens with a constant ligament length (about 3 mm). The tests were carried out at room temperature with an instrumented impact pendulum (Ceast) at a test speed of 3.7 m/s. The total work of fracture was divided by the cross-sectional area. It should be noted that the test direction was the same as in the low-speed tensile tests but transversal to that of the Izod impact test.

The morphology of the fracture surfaces of the DDENT specimens generated in the tensile tests with low speed and tensile impact tests was char-

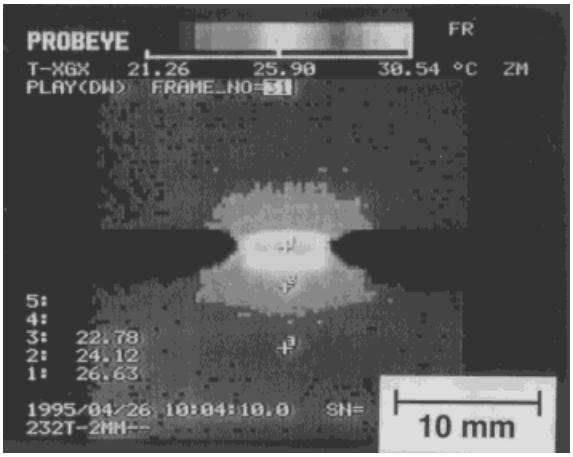

Figure 2 Infrared thermograph picture of sample 2 (PA6/PP/Comp. 72/18/10) at position 3.

acterized with a JEOL JSM 5400 scanning electron microscope to be able to determine the changes in morphology of the different blends during the tests and to evaluate the fracture mechanisms. For reference, the morphology of untested specimens was studied after fracturing in liquid nitrogen.

During the low-speed tensile measurements, infrared thermography (IT) was applied and IT pictures were taken (Figure 2, as in ref. 24). These studies showed the plastic zone to be elliptical in shape.

Essential Work of Fracture Procedure

In the essential work of fracture procedure,[26] the total work of fracture is divided into two parts: the work related to the tip of a crack and that related to the outer region. The crack tip specific work, the essential work of fracture (w_e), is a material property for a given sheet thickness and thus is a measure of toughness. The nonessential work done in the outer region depends on the shape of the plastic zone surrounding the crack and is related to the plastic work dissipation per unit volume of the material (w_p).

The total energy to failure (W_f) is given by the expression

$$W_f = w_e lt + w_p \beta l^2 t \qquad (1)$$

where l is the ligament length, t is the sheet thickness, and β is a shape factor associated with the plastic zone [Fig. 1(b)]. Normalizing by lt, we obtain

$$w_f (= W_f/lt) = w_e + w_p \beta l \qquad (2)$$

For determination of the essential work of fracture, the total energy to failure per unit area of the ligament for a DDENT specimen (w_f) is plotted versus ligament length (l). The least-squares regression line is fitted to the data, and the slope and the intersection with the y axis ($=w_e$), together with the correlation coefficient, are determined.

For determination of the plastic work dissipation per unit volume of the material, the zone height (h) of the sample is plotted versus ligament length (l). The dimension h defines the maximum extent of the necked region, i.e., the region in which the thickness is reduced in the direction of the applied stress. The plot should be a line passing through the origin, but in practice, it often passes close to rather than through the origin. The gradient is proportional to the shape factor β, as set out in eq. (1). The constant of proportionality (β) depends on the shape of the zone, which may be circular, elliptical, or diamond shaped.

$$\text{circular zone: } \beta = \pi/4 \qquad (3)$$

$$\text{elliptical zone: } \beta = \pi h/4l \qquad (4)$$

$$\text{diamond-shaped zone: } \beta = h/2l \qquad (5)$$

The gradient of the plot of w_f versus l is βw_p, and that of h versus l in the case of an elliptical zone is $4\beta/\pi$. The plastic work dissipation per unit volume (w_p) for samples exhibiting the elliptical zone is then given by the expression

$$w_p = (4/\pi)*(\text{gradient of } w_f \text{ vs. } l/\text{gradient of } h \text{ vs. } l) \qquad (6)$$

The recommended range of the ligament length is $3t < l < w/3$, where w is the specimen width.[26] When the total work of fracture is determined, the load-deformation curves for the different ligament lengths should be identical in form (see Fig. 6). Furthermore, complete deformation of the plastic zone before crack growth is a basic requirement of the procedure.

RESULTS AND DISCUSSION

Tensile and Impact Properties

Elastic modulus, tensile strength, and notched Izod impact strength of the blends containing PA6

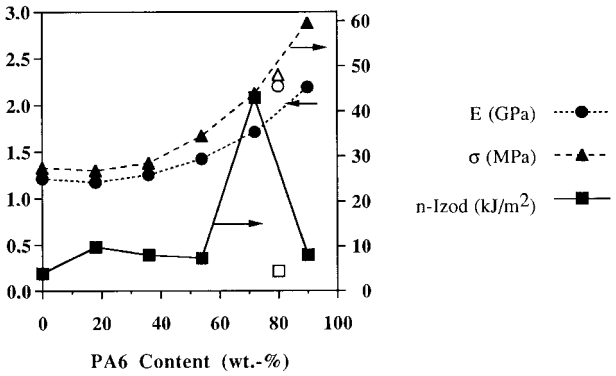

Figure 3 Elastic modulus (E), tensile strength (σ), and notched (n) Izod impact strength for (black symbols) PA6/PP blends compatibilized with 10 wt % SEBS-*g*-MA and (white symbols) a noncompatibilized reference composition.[6,8]

and PP with 10 wt % of SEBS-*g*-MA are presented in Figure 3; synergistic behavior is observed for the compatibilized blend with a PA6/PP weight ratio of 80/20. Mechanical properties of this particular blend composition indicate a favorable combination of toughness, strength, and stiffness (i.e., notched Izod impact strength = 43 kJ/m^2, σ = 44 MPa, and E = 1.7 GPa).[6–8]

SEM micrographs in Figure 4 show the effect of compatibilization at the tough composition (PA6/PP ratio of 80/20). The addition of 10 wt % of the SEBS-*g*-MA compatibilizer made the blend morphology highly homogeneous. Further studies by TEM[7,8] revealed that, in this supertough composition, not only PA6 but also the elastomeric compatibilizer formed a continuous phase. PP, in turn, existed as a fine dispersion with an average particle size of 0.4–1 μm. At lower PA6 contents, agglomerated elastomeric particles with PA6 inclusions were embedded in the continuous PP matrix. Phase inversion in the compatibilized blends thus took place between the PA6/PP weight ratios of 60/40 and 80/20. This may have some relevance for the results reported below as well.

Fracture Mechanical Studies

In the fracture mechanical studies, the results for the tough compatibilized blend composition with a PA6/PP ratio of 80/20 were compared with those for the corresponding PA6/PP 60/40 blend and for PA6 with the same amount of SEBS-*g*-MA added. The noncompatibilized 80/20 blend was studied as a reference.

Tensile Tests with Slow Speed

Tensile tests were carried out by applying the essential work of fracture concept as described above. The results, representing three different sample positions of the four blend compositions, are presented in Table I.

For the noncompatibilized PA6/PP (80/20) blend, the plastic work of fracture (w_p) was observed to vary widely with the sample position. The essential work of fracture (w_e), in contrast, remained reasonably constant (Fig. 5). It must be noted here that even a fairly brittle material such as the noncompatibilized PA6/PP (80/20) blend behaved in a manner (identical shape of the measured load-deflection curves) that allowed the total work of fracture procedure to be applied at slow speed.

As shown in Figure 4, the noncompatibilized blend exhibited coarse morphology, and the differences recorded in the plastic work suggest that this coarse morphology is not stable during injection molding. High shear forces during the injection stage and fast cooling of the surface region cause orientation of the dispersed phase, leading

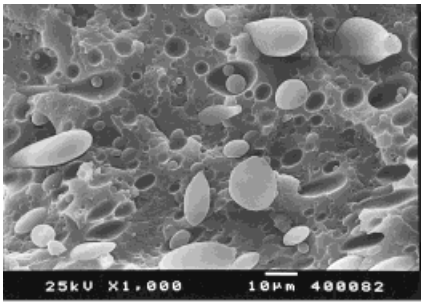

(a)

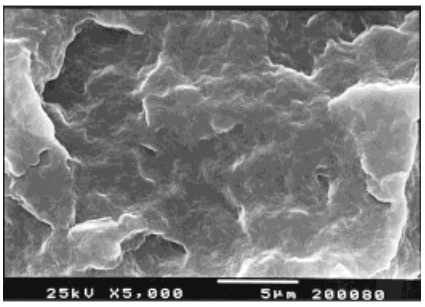

(b)

Figure 4 SEM micrographs of the cryogenically fractured surfaces of (a) a noncompatibilized and (b) a compatibilized (10 wt % SEBS-*g*-MA) blend with a PA6/PP ratio of 80/20.

to anisotropic morphology, as observed for many polymers and blends.[4,11,29,30] Here we found that when the orientation of the matrix and the dispersed phase was parallel to the testing direction (L samples), significant deformation occurred in the surface or skin region. This deformation affected the stress–strain behavior so that a tail was formed in the curve, which in turn affected the values of w_e and w_p [Fig. 6(b)]. Therefore, when a large deformation of the skin was observed, the essential work of fracture or the plastic work dissipation could not be reliably determined. Hence, the results we report describe T samples (transversal to the flow direction), which showed fewer such problems.

Similar deformation of the skin region during testing was observed with blend 1 (PA6/PP/Comp. 54/36/10), and it increased from position 1 to position 3. For samples with different ligament lengths representing positions 1 and 2, the effect of the tail was small and could be neglected. For the samples taken from position 3, however, deformation of the skin was marked, and it was impossible to separate this effect from the essential and plastic work. Position 3 was therefore ignored. Deformation of the skin affected the essential and plastic work of the PA6/PP/Comp. 54/36/10 blend at position 2 as well. We assumed that because deformation of the skin was observed for a blend with a continuous PP phase, it must have been this morphology that caused a high deformation of the skin in the T samples as well.

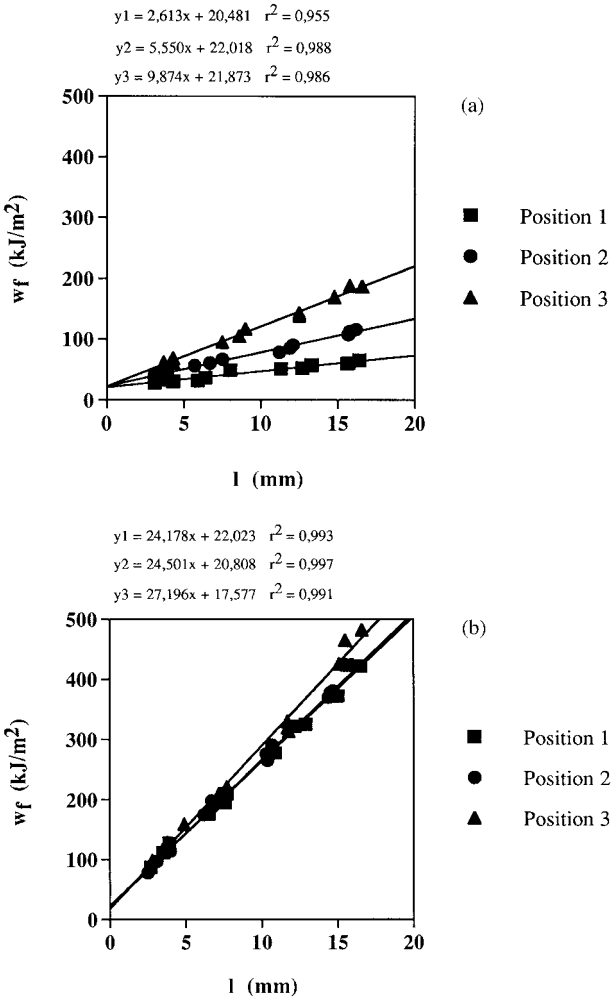

Figure 5 Total work of fracture per unit area (w_f) versus ligament length (l) for samples representing different positions of (a) noncompatibilized (blend 2A) and (b) compatibilized blend (blend 2) with a PA6/PP ratio of 80/20.

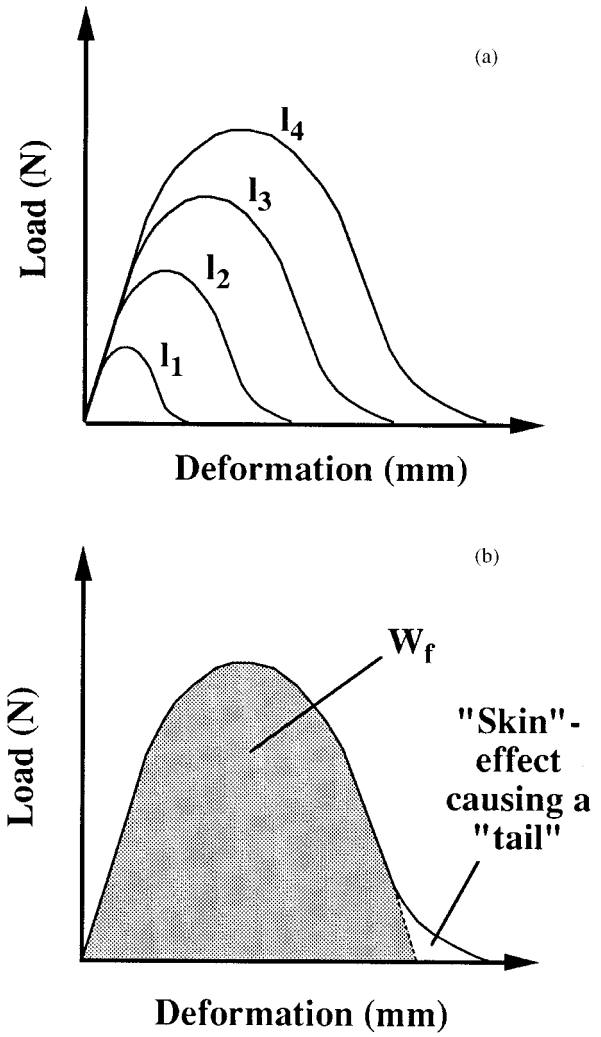

Figure 6 Schematic figures showing (a) load-deformation curves for different ligament lengths and (b) the effect of skin deformation on the shape of the curve (tail formation).

Comparison of Figure 5(a) and (b), which present the results for the noncompatibilized and the compatibilized blends with a PA6/PP ratio of 80/20, shows that compatibilization decreases the effect of the position with respect to the plastic work of fracture. Evidently, the more stable morphology of the compatibilized blend is less affected by the subsequent processing. In contrast to the differences in plastic work dissipation, the essential work of fracture (w_e) was about 21 kJ/m^2 in both cases. This indicates that the toughening induced by compatibilization that was observed in impact tests was caused by plastic deformation processes such as shear yielding and crazing.

Figure 7 shows the essential work of fracture and the plastic work dissipation for all of the blends examined (position 1). As can be seen, both w_e and w_p increased with PA6 content. Whereas w_e increased steadily as a function of the amount of PA6, w_p increased sharply when the PA6 content was increased from 54 to 72 wt %. Again, the increase of w_p induced by compatibilization was very significant. Comparing these results with the results of the basic mechanical tests shown in Figure 1, it would seem that the essential work of fracture correlates with tensile strength and that the plastic work dissipation shows some correlation with impact strength. However, the kind of peak observed for the PA6/PP/Comp. 72/18/10 blend in the high-speed impact test (notched Izod) was not observed in the low-speed tensile fracture mechanical test. This difference in behavior could be due to the difference in the testing speed, the testing mode (tensile versus bending), or both.

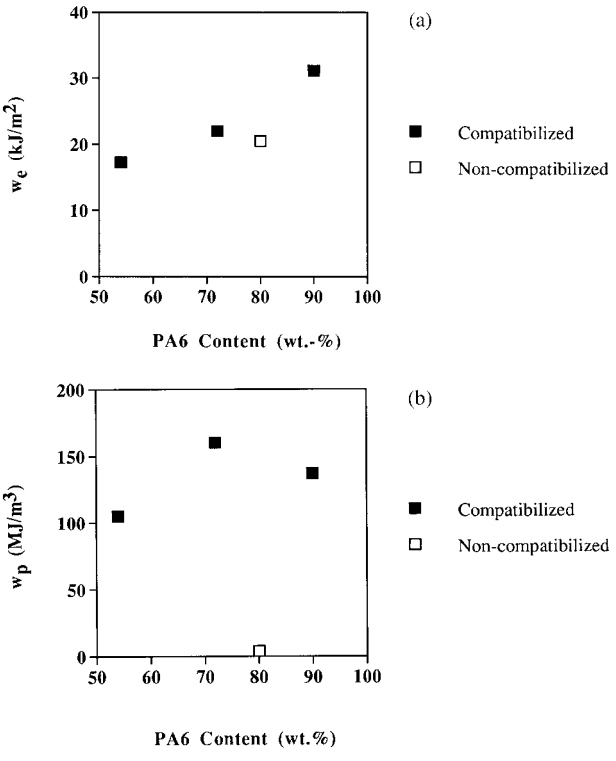

Figure 7 (a) Essential work of fracture (w_e) and (b) plastic work of fracture (w_p) versus PA6 content.

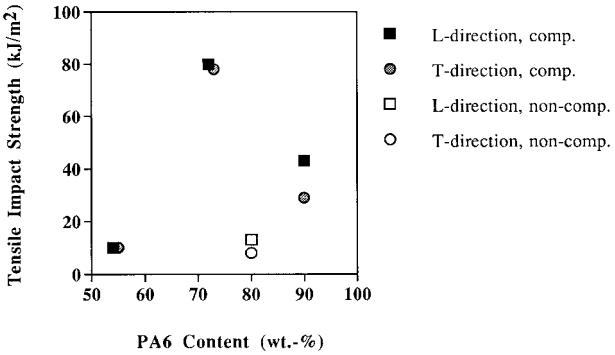

Figure 8 Tensile impact strength versus PA6 content of DDENT specimens tested in both *T* and *L* directions. comp, compatibilized; non-comp., noncompatibilized.

Tensile Impact Tests

The essential work of fracture procedure was not applied in the tensile impact tests. The effect of the high testing velocity was instead evaluated by the work of fracture determined for DDENT specimens with a constant ligament length (Fig. 8).

The high-speed tensile impact loading revealed striking differences in the fracture behavior of the four blends. Although the findings are not demonstrated here, we suppose that these differences are related to the effects of the plastic work of fracture. Such a trend, increased w_p with increasing test speed (w_e remained constant), was observed by Karger-Kocsis and Czigany for unfilled and filled poly(ethylene terephthalate)(PET).[24] Although both the test mode and the direction were different, the results of our tensile impact tests correlated well with those of the Izod tests on single-notched samples. However, the tensile impact tests gave somewhat higher values. Evidently, during impact, the skin region participates in the fracture process, because remnants of highly elongated skin were observed on the fracture surface. Because the thickness of the DDENT specimens was only 2 mm, the "skin effect" may have been considerable. These factors

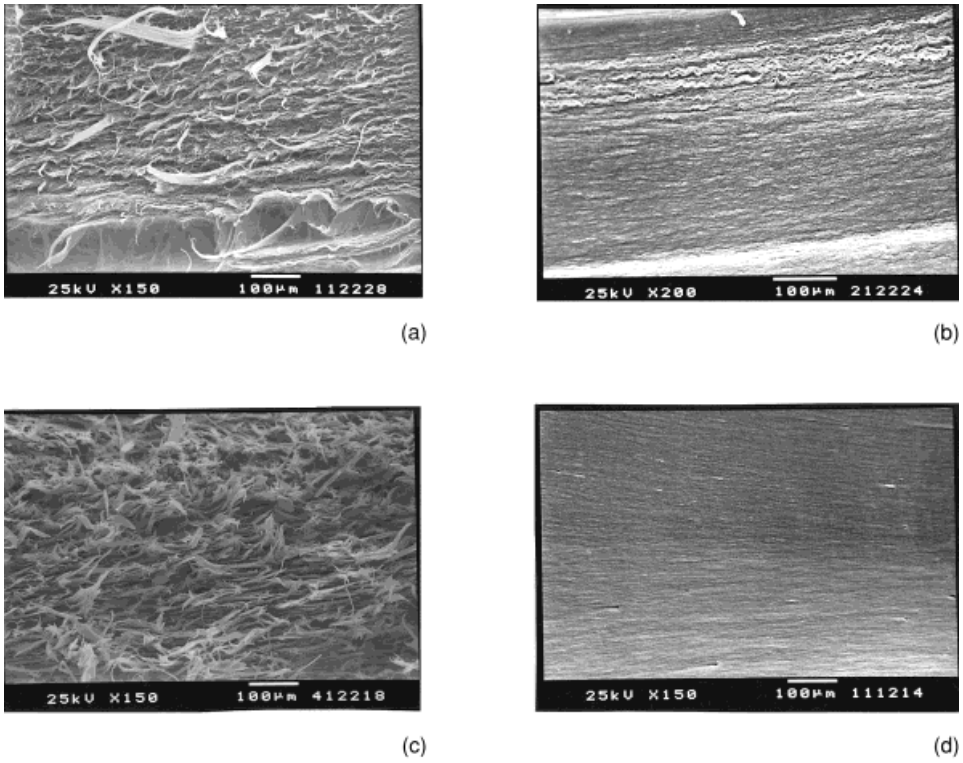

Figure 9 Fracture surfaces generated in the low-speed tensile test of (a) blend 1, (b) blend 2, (c) blend 2A, and (d) blend 3 (T direction, position 2, l = 8 mm).

increased the work of fracture, particularly in the L direction, where the orientation of the skin was parallel to the testing direction.

Morphology of Fracture Surfaces

Tensile Tests with Low Speed

SEM micrographs of the fracture surfaces generated in the tensile tests with low test speed (2 mm/min) are presented in Figure 9. Morphological analysis revealed clear differences between the four blend compositions. The noncompatibilized reference blend (2A) exhibited a very unhomogeneous fracture surface, indicating poor adhesion between the PP and PA6 phases. Somewhat similar behavior was found for blend 1 (composition 54/36/10), but it contained fewer and finer fibrils than the noncompatibilized blend.

The two PA-rich compositions in turn exhibited much smoother fracture surfaces, suggesting more ductile behavior. The tough blend composition (blend 2) showed a narrow region of very fine curly fibrils between the smooth center and the skin region. PA6 modified with 10 wt % of the elastomeric compatibilizer (blend 3) exhibited the smoothest fracture surface, suggesting very ductile failure behavior in this low-speed test. Higher magnifications revealed some indication of cavitation caused by the fine rubber dispersion of droplet size below 1 μm.

SEM studies on specimens fractured in the low-speed tensile test elucidated the differences in the fracture behavior of the four blends. In agreement with the observations of Gonzales-Montiel et al.,[16] no signs of cavitation were found.

Effect of sample position (Fig. 1) on the morphology of the fracture surfaces was studied with the noncompatibilized brittle PA6/PP 80/20 blend (blend 2A). Basically, the morphologies were closely similar, but enhanced fibrillation of the PA6 matrix was observed at positions 2 and 3 relative to position 1. At position 1, the material was less deformed, as was also suggested in the fracture mechanical analysis. Comparison of the different materials should thus be made with samples representing this position. Effect of ligament length on the morphology of the fracture surfaces was studied with the ductile blend 2, but no significant effect was found.

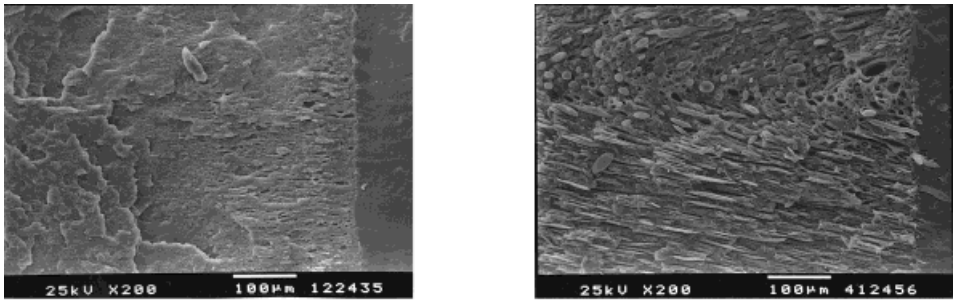

Figure 10 Fracture surfaces generated in the tensile impact test of (a) blend 1 (*L* direction) and (b) blend 2A (*T* direction); the notch is seen on the right.

Tensile Impact Tests

The fracture surfaces generated in a high-speed tensile impact test differed from those obtained in the tensile test with low speed (2 mm/minute). The differences between the four blend compositions became more evident in the tensile impact test.

The noncompatibilized blend (blend 2A) exhibited very coarse two-phase morphology with a clear skin/core structure which was little deformed in the tensile impact test relative to the low-speed tensile test. The layered structure consisted of highly deformed skin (thickness about 200 μm), an intermediate layer with deformed PP platelets, and a core with slightly elliptical droplets [Fig. 10(b)]. The large platelets exhibited huge deviation in size, from some tens to several hundred micrometers, and the adhesion between the phases was poor. Differences between the *L* and *T* directions were small, with more deformed platelets or fibers in the *T* direction.

The relatively smooth fracture surface of blend 1, with no signs of plastic deformation, suggested brittle failure in the high-speed test. A narrow slightly deformed region near the crack tip was found in the *L* direction [Fig. 10(a)], but otherwise, there were no differences between the *L* and *T* directions.

The fracture surfaces of blends 2 and 3 differed totally from those of blends 1 and 2A (Fig. 11). These blends exhibited large-scale plastic deformation, suggesting ductile behavior in failure as discussed above. No clear differences between *L* and *T* directions were evident for blend 2. At higher magnifications, a dispersion of PP droplets from 0.3 μm to a few micrometers in diameter could be seen. Probably, these tiny PP droplets acted as initiators for cavitation [Fig. 11(c)]. Blend 3 showed even more obvious large-scale plastic deformation [Fig. 11(b)], which was related to the very ductile fracture behavior. Tiny droplets of the order of 0.2–0.5 μm showing signs of cavitation were found at higher magnifications [Fig. 11(d)]. A denser deformation pattern indicating greater toughness was seen in the *T* direction, while there was a small smooth region close to the notch in the *L* direction.

Comparison of blends 2 and 3 showed these two tough materials to exhibit similar large-scale plastic deformation, but the microscale deformation was slightly coarser for blend 2. The greater coarseness is probably due to the slightly larger particle size of the dispersed PP phase (about 1 μm) than of the neat elastomer droplets (0.2–0.5 μm) within the PA6 matrix. Compared with these two compositions, blend 1 (PA6/PP/Comp. 54/36/10) exhibited more brittle failure both in micro and in macro scale, and it showed slightly coarser morphology with no signs of cavitation but two phases well attached to each other. From earlier studies,[7,8] it seems clear that at this composition, PP forms the matrix, and this may be the reason for the more brittle failure.

The effect of compatibilization (material 2 vs. 2A) was seen as an extremely fine stabilized morphology maintained in the failure. Thanks to this morphology, the fracture behavior changed from very brittle to ductile and the effect of the testing direction was diminished in the compatibilized blend.

SEM studies on the tensile impact–tested specimens were in good agreement with the results of the tests discussed above. However, the SEM micrographs do not allow detailed characterization of the fracture mechanisms. It seems that the tough blend compositions undergo both plastic

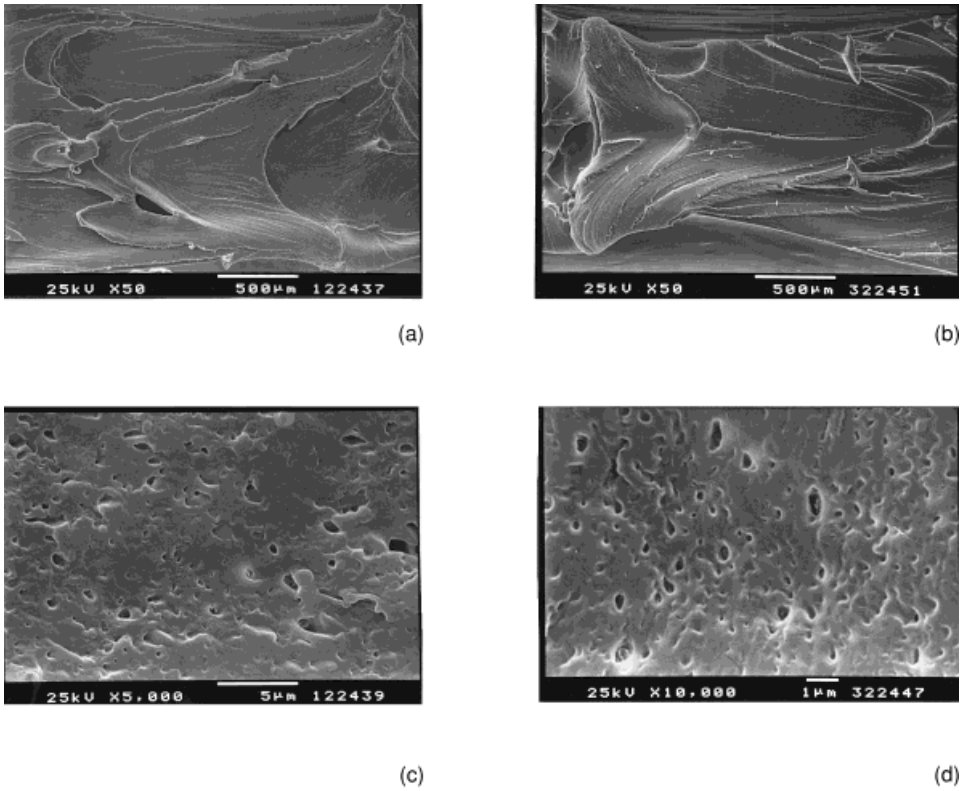

Figure 11 Fracture surfaces generated in the tensile impact test of (a) blend 2 and (b) blend 3; examples of higher magnifications are shown in (c) blend 2 and (d) blend 3.

deformation of the matrix and cavitation of the dispersed phase. Gonzales-Montiel et al.[16] have studied the fracture behavior of PA6/PP blends containing 20 wt % SEBS-*g*-MA by impact tests on single-edge notched samples. They found cavitation of rubber particles in binary blends of PA6 and 20 wt % SEBS-*g*-MA, and no cavitation but extensive shear yielding of both the PA6 and the PP phases in PA6/PP 80/20 blends with 20 wt % SEBS-*g*-MA. On the basis of studies on PP-rich PA6/PP blends, Rösch and Mülhaupt[17] suggest that several mechanisms may be acting, depending on the blend morphology. When the dispersed PA6 droplets are surrounded by more flexible material, this soft shell undergoes plastic deformation (shell cavitation) before extensive yielding of the PP matrix. In our case, the tough PA6/PP blend (blend 2) exhibited complex morphology with tiny PA6 inclusions surrounded by a continuous elastomer phase, while PP formed larger dispersed droplets (about 0.4–1 μm).[7,8] It is thus probable that the discrete PP droplets induce cavitation at the interfaces and the cocontinuous PA6 and SEBS-*g*-MA phases undergo plastic deformation.

Evaluation of the Method

The essential work of fracture procedure has been applied successfully for "tough" polymers and blends where the plastic deformation is greater than that allowed by the linear elastic fracture mechanical concept.[22,23,25,27] It should be mentioned here that determinations of the height of the plastic zone (h) and the shape (round, elliptical, or diamond) of the plastic region needed to calculate β and w_p are not straightforward, and errors may be expected in some cases. As recommended in the ESIS protocol,[26] therefore, w_p should be determined from the total energy per unit volume required to deform a uniaxial tensile sample to failure with the same test speed. Even though not all of the ligament lengths were in the recommended region ($3t < 1 < w/3$, or between 6 and 8 mm), the identical shape of the measured load-deflection curves justified the ligament lengths used (4–12 mm).

The values of w_e obtained in this study for the PP-rich blend (composition 1) are close to those for PP (4.3–5.8 kJ/m^2), and the values for the PA-rich blends are close to those for toughened

PA (30 kJ/m^2).[27] As stated elsewhere, the values of w_e may in some cases be affected by blend (or polymer) microstructure and, as shown also in this article, by the position where the specimen was taken.[24] The importance of the position can be explained by the "skin" effect, even though this was minimized by "correcting" the load-deformation curve. The similar w_e values of the compatibilized and noncompatibilized blends suggest that w_e is not a very good indicator of blend "toughness." Our results rather suggest that the term $\beta^* w_p$ (or when β is known, w_p) describes much better the "toughness" of a particular polymer or blend that is introduced by micromechanical processes such as crazing, cavitation, or shear yielding.[28] In addition, it must be noted that an increase in the testing speed can have a considerable effect in comparisons of the toughness of different materials. Looking at the difference in toughness between blends 2 and 3 under static loading, we see that composition 2 (in position 1) had a 21% higher w_p value, but under impact conditions, the total work of fracture was 100% higher. This observation emphasizes that, in working to optimize the toughness of polymeric materials, the test conditions (here, velocity) should be close to the expected loading velocity in the application of the material.

CONCLUSIONS

The essential work of fracture procedure was applied to characterize the fracture mechanics of noncompatibilized PA6/PP blends and the same blends compatibilized with SEBS-*g*-MA. The following conclusions are drawn. First, the essential work of fracture procedure, previously used for thin films, can be applied to injection-molded tough blends as well, even though the considerable skin deformation distorts the values of the total work of fracture (w_f). A "tail" in the load-deformation curve caused by the skin effect must be neglected in the determination of the essential (w_e) and plastic (w_p) work of fracture. Second, the plastic work of fracture (w_p) correlates with impact strength, and the essential work of fracture (w_e) correlates with tensile strength. Hence, w_p represents the "toughness" of these materials better than w_e does, even though w_p is not a material parameter and is slightly affected by the sample position. Finally, the testing speed considerably affects the ordering of the blends in terms of "toughness," because of differences in the micromechanical failure mechanisms; e.g., SEM revealed no signs of cavitation for the PA6/PP/SEBS-*g*-MA 72/18/10 and 90/0/10 blends at low testing speed, but cavitational processes seemed to occur in impact test conditions.

This work was supported by funding received from the Finnish Academy, Technology Development Center of Finland (TEKES) and Deutscher Akademischer Austausch Dienst (DAAD). Prof. J. Karger-Kocsis is thanked for helpful discussions.

NOMENCLATURE

DDENT	deeply double-edge notched tension
HDPE	high-density polyethylene
IT	infrared thermography
LEFM	linear elastic fracture mechanics
PYFM	plastic or postyield fracture mechanics
PA	polyamide
PP	polypropylene
PET	poly(ethylene terephthalate)
SEBS-*g*-MA	poly(styrene-*block*-(ethylene–butylene)-*block*-styrene copolymer grafted with maleic anhydride
SEM	scanning electron microscopy
TEM	transmission electron microscopy

SYMBOLS

β	shape factor; see eqs. (1–5)
E	tensile modulus (GPa)
h	zone height (mm)
l	ligament length (mm)
σ	tensile strength (MPa)
t	sheet thickness (mm)
w_e	essential work of fracture (kJ/m^2); see eqs. (1) and (2)
w_f	total work to failure per unit area of the ligament for a DDENT specimen (kJ/m^2); see eq. (2)
W_f	total work of fracture (J); see eq. (1)
w_p	plastic work dissipation per unit volume of the material (MJ/m^3); see eqs. (1), (2), and (6)

REFERENCES

1. L. A. Utracki, *Polymer Alloys and Blends,* Carl Hanser Verlag, New York, 1990.

2. F. Ide and A. Hasegawa, *J. Appl. Polym. Sci.,* **18,** 963 (1974).
3. G. Jordhamo, J. Manson, and L. Sperling, *Polym. Eng. Sci.,* **26,** 517 (1986).
4. M. Heino, *Acta Polytechnica Scandinavica, Chemical Technology and Metallurgy Series,* No. 220 (1994), Dr. Tech. Dissertation, The Finnish Academy of Technology, 49 p.
5. M. Heino and T. Vainio, in *Handbook of Applied Polymer Processing Technology,* N. P. Cheremisinoff and P. N. Cheremisinoff, Eds., Marcel Dekker, Inc., New York, 1996, Chap. 7, pp. 233–263.
6. R. Holsti-Miettinen, J. Seppälä, and O. Ikkala, *Polym. Eng. Sci.,* **32,** 868 (1992).
7. R. Holsti-Miettinen, J. Seppälä, O. Ikkala, and I. Reima, *Polym. Eng. Sci.,* **34,** 395 (1994).
8. O. Ikkala, R. Holsti-Miettinen, M. Heino, et al., *Polymer,* to appear.
9. P. Hietaoja, R. Holsti-Miettinen, J. Seppälä, and O. Ikkala, *J. Appl. Polym. Sci.,* **54,** 1613 (1994).
10. T. Vainio and J. Seppälä, *Polym. Polym. Compos.,* **1,** 427 (1993).
11. R. Holsti-Miettinen, M. Heino, K. Perttilä, and J. Seppälä, *J. Appl. Polym. Sci.,* **58,** 1551 (1995).
12. J. Rösch and R. Mülhaupt, *Makromol. Chem., Rapid Commun.,* **14,** 503 (1993).
13. J. Rösch and R. Mülhaupt, *Polym. Bull.,* **32,** 697 (1994).
14. A. Gonzales-Montiel, H. Keskkula, and D. R. Paul, *Polymer,* **36,** 4587 (1995).
15. A. Gonzales-Montiel, H. Keskkula, and D. R. Paul, *Polymer,* **36,** 4605 (1995).
16. A. Gonzales-Montiel, H. Keskkula, and D. R. Paul, *Polymer,* **36,** 4621 (1995).
17. J. Rösch and R. Mülhaupt, *J. Appl. Polym. Sci.,* **56,** 1607 (1995).
18. S. Wu, *Polymer,* **26,** 1855 (1995).
19. R. Borggreve, R. Gaymans, J. Schuijer, and J. Ingen Housz, *Polymer,* **28,** 1489 (1987).
20. C. Bucknall, *Toughened Plastics,* Applied Science, London, 1977.
21. G. Michler, *Kunststoff-Mikromechanik,* Carl Hanser Verlag, München, 1992.
22. A. G. Atkinson and Y.-W. Mai, *Elastic and Plastic Fracture,* Ellis Horwood, Chichester, 1988.
23. J. G. Williams, *Fracture Mechanics of Polymers,* Ellis Horwood, Chichester, 1987.
24. J. Karger-Kocsis and T. Czigany, *Polymer,* **37,** 2433 (1996).
25. W. Y. F. Chan and J. K. Williams, *Polymer,* **35,** 1666 (1994).
26. A. Gran, *Testing Protocol for Essential Work of Fracture,* European Structural Integrity Society (ESIS), TC-4, Les Diableres, Switzerland, 1993.
27. J. Karger-Kocsis, in *Application of Fracture Mechanics to Composite Materials,* K. Friedrich, Ed., Elsevier, Amsterdam, 1989.
28. J. Karger-Kocsis, *Polym. Eng. Sci.,* **36,** 203 (1996).
29. T. Harmia and K. Friedrich, *Comp. Sci. Techn.,* **53,** 423 (1995).
30. L. A. Utracki and M. M. Dumoulin, in *Polypropylene: Structure, Blends and Composites, Vol. 2, Copolymers and Blends,* J. Karger-Kocsis, Ed., Chapman and Hall, London, 1995.